

## 5. THE DISTRIBUTION OF THE PLATINUM GROUP ELEMENTS AND GOLD

---

### 5.1. Introduction

Noble metals are normally present at trace element levels in both the crust and mantle, but may become concentrated by several distinct processes. The most important of these is segregation of immiscible sulphide melt from a silicate magma, and collection of the highly chalcophile noble metals by the sulphide melt (Barnes and Maier, 1999 and references therein). In addition, Os, Ir, Ru (the IPGE) and Rh may possibly be concentrated by chromite (Capobianco *et al.*, 1994), Ir by olivine (Bürgmann *et al.*, 1987), the IPGE, Rh and Pt by PGM crystallising directly from the silicate magma (Brenan and Andrews, 2001), and Os, Ir and Pt by atomic metal clusters (Tredoux *et al.*, 1995). In view of this, the PGE are important elements in deciphering the petrogenesis of mafic-ultramafic igneous rocks.

### 5.2. Results

The concentrations of the PGE and Au in the analysed samples are listed in Appendix II. The metals are plotted versus stratigraphic height in Figure 5.1. It is seen that there is a broad general decrease in PGE concentration with height through the Complex. A minor compositional break is visible in the lower part of the MHZBG at about 790m, where PGE levels decrease markedly. In addition, there is a sharp decrease in PGE concentration within the uppermost portion of the PXT so that the uppermost two Gabbroic Units have markedly lower PGE concentrations than the underlying rocks. Finally, the UGAB appears to have higher PGE concentrations than the GN.

Figure 5.2. shows Pd/Ir and Pt/Pd ratios plotted versus height. It is evident that the Pd/Ir ratio decreases from the base of the Complex towards the top of the MHZBG, before a sharp increase at the base of the PXT is followed by progressively higher values towards the top of the Complex. This is the opposite of what is observed in other layered intrusions such as the Bushveld Complex (Maier and Barnes, 1999), where Pd/Ir increases with height. The reason for this pattern is that Pd/Ir is a crude

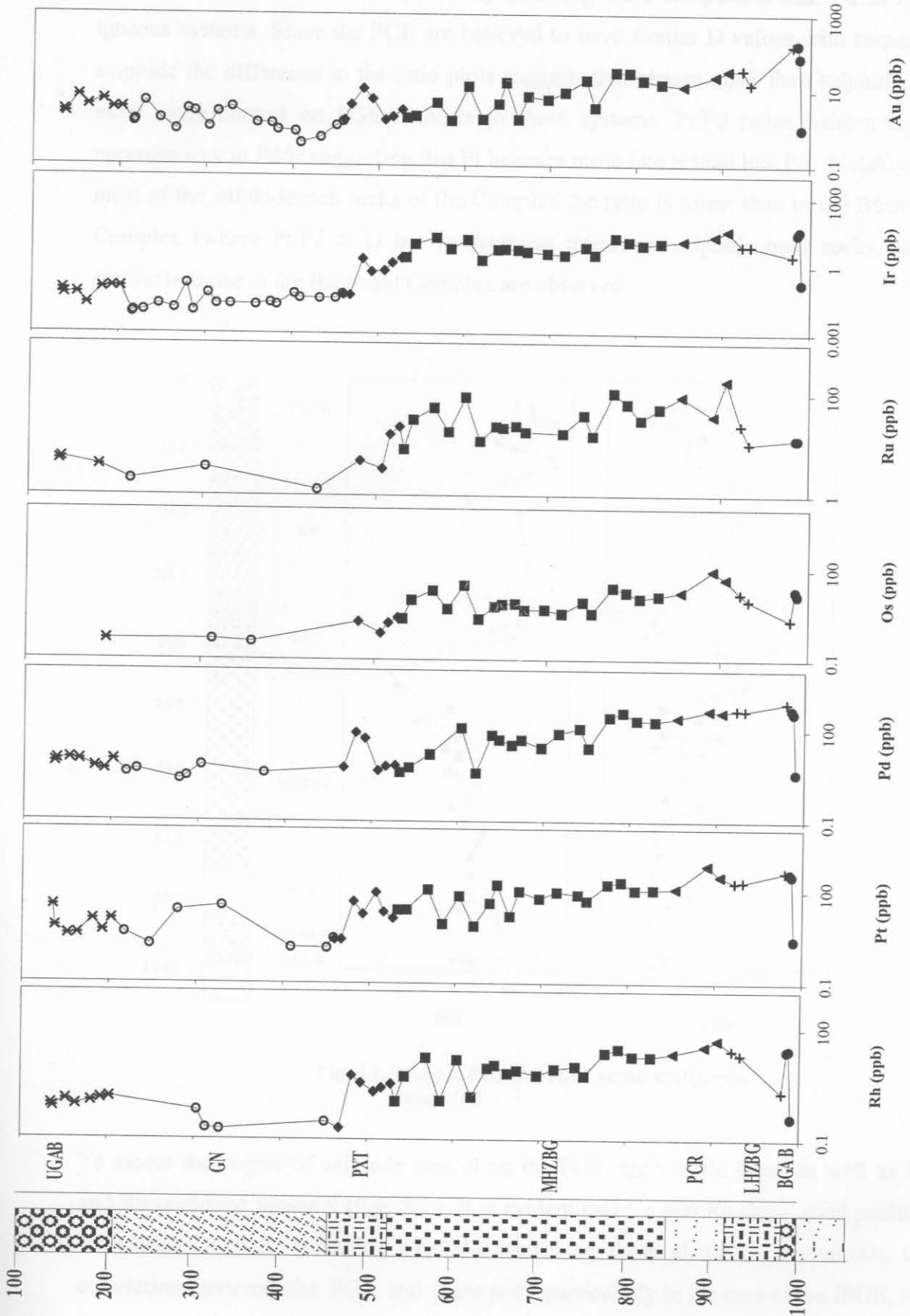


Fig. 5.1. Concentration of PGE and Au plotted versus stratigraphic height (m).

differentiation index, with Ir apparently behaving more compatible than Pd in many igneous systems. Since the PGE are believed to have similar D values with respect to sulphide the difference in the ratio plots suggests that phases other than sulphide also exert some control on PGE contents in these systems. Pt/Pd ratios behave in the opposite way to Pd/Ir suggesting that Pt behaves more like Ir than like Pd. Notably, for most of the sulphide-rich rocks of the Complex the ratio is lower than in the Bushveld Complex (where  $Pt/Pd > 1$ ) but in the most primitive, sulphide poor rocks, ratios similar to those in the Bushveld Complex are observed.

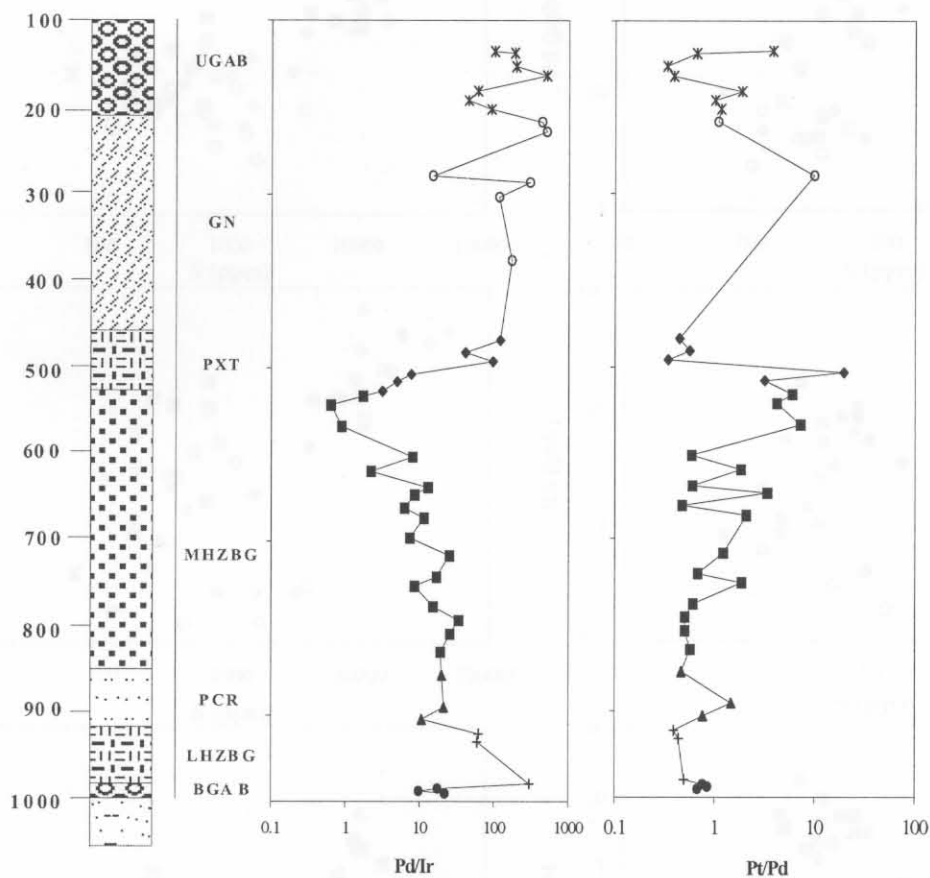


Fig. 5.2. Ratios of Pd/Ir and Pt/Pd versus stratigraphic height (m)

To assess the degree of sulphide control on the PGE, each noble metal as well as Cu and Re is plotted versus S (Fig. 5.3.). It is evident that Cu and Re show good positive correlations with S, indicating sulphide control on these elements. In contrast, the correlation between the PGE and S are poor, particularly in the case of the IPGE, Rh

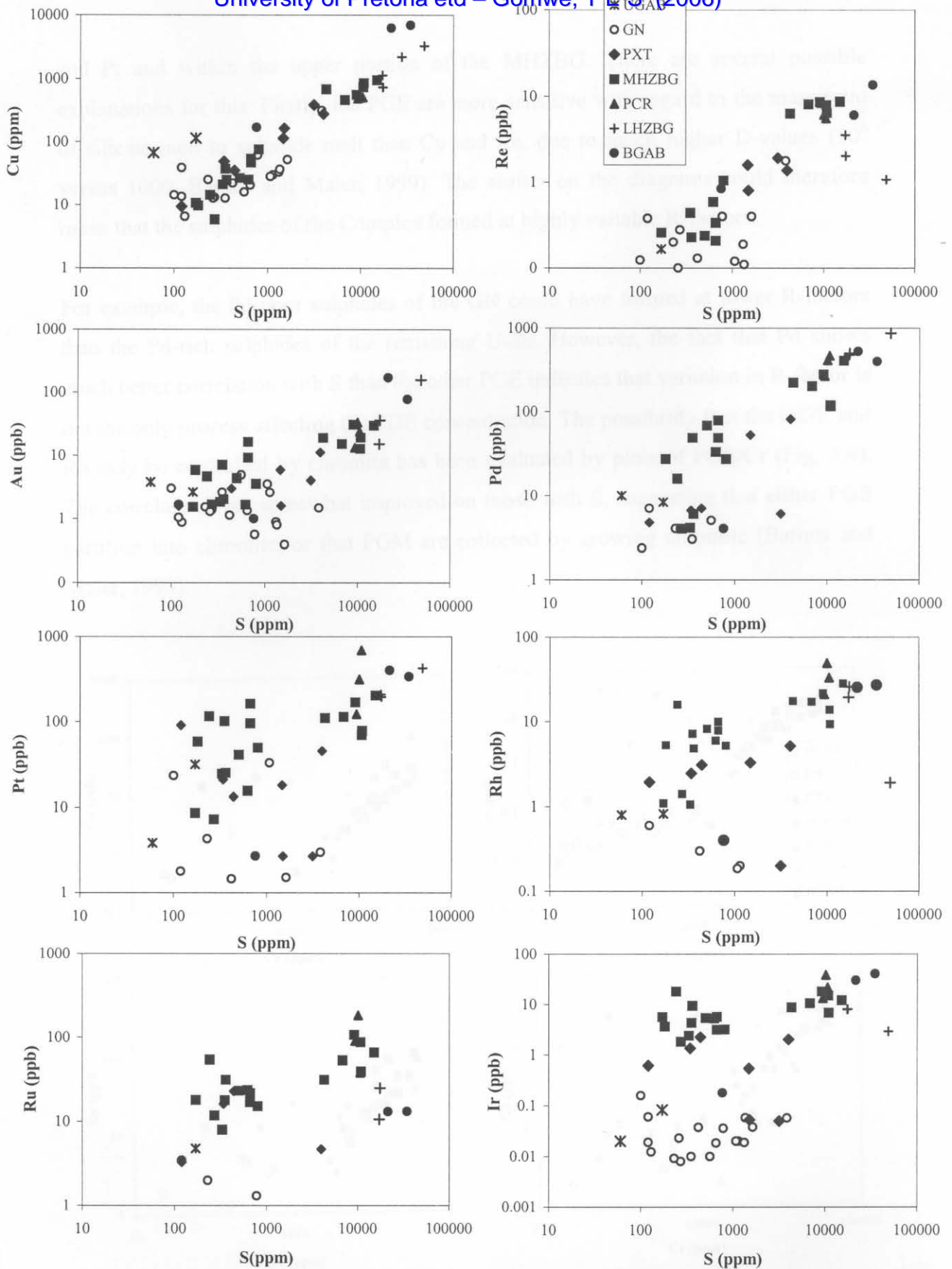


Fig 5.3. Variation diagrams of PGE, Cu and Re versus S.

and Pt and within the upper portion of the MHZBG. There are several possible explanations for this. Firstly, the PGE are more sensitive with regard to the mass ratio of silicate melt to sulphide melt than Cu and Re, due to much higher D-values ( $10^6$  versus 1000, Barnes and Maier, 1999). The scatter on the diagrams could therefore mean that the sulphides of the Complex formed at highly variable R-factors.

For example, the Pd-poor sulphides of the GN could have formed at lower R-factors than the Pd-rich sulphides of the remaining Units. However, the fact that Pd shows much better correlation with S than the other PGE indicates that variation in R-factor is not the only process affecting the PGE concentration. The possibility that the IPGE and Rh may be controlled by chromite has been evaluated by plots of PGE/Cr (Fig. 5.4). The correlations are somewhat improved on those with S, suggesting that either PGE partition into chromite, or that PGM are collected by growing chromite (Barnes and Maier, 1999).

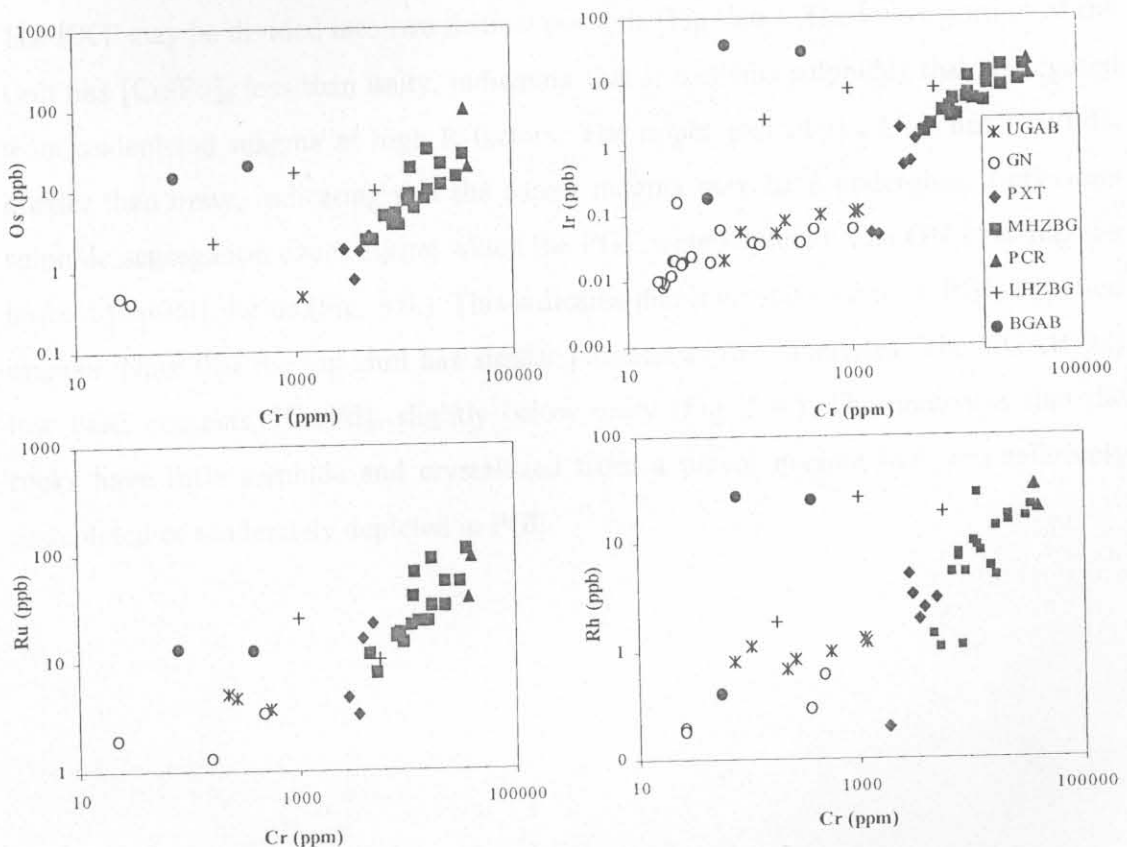


Fig. 5.4. Variation diagrams of IPGE versus Cr.

### 5.3. Spider plots

The noble metal concentrations are normalized to model mantle and plotted in order of increasing melting temperature in Figure 5.5. Nickel, Cu and Au are added to the graph due to their broadly similar behaviour to PGM's during fractionation. Several features are highlighted. The BGAB has relatively fractionated PGE patterns, with a progressive increase from Ni to Cu.  $[Cu/Pd]_n$  is  $>1$ . Such a pattern may be expected to represent sulphides that segregated from undepleted magma at relatively low R factors, at which the difference in partitioning between the PGE and Cu or Ni is swamped by the large amount of sulphides. The LHZBG, PCR and Lower MHZBG have different patterns, in that  $[Cu/Pd]_n$  is largely less than unity, indicating that the sulphides of these Units segregated at high R-factors. The remainder of the MHZBG has relatively flat patterns with  $[Cu/Pd]_n$  at less than unity indicating the presence of cumulus PGE, but the relatively high IPGE/PPGE ratio suggests partial control of the PGE by either monosulphide solid solution (mss) or PGM.

The PXT may be divided into two distinct portions (Fig. 5.6.). The lower portion of the Unit has  $[Cu/Pd]_n$  less than unity, indicating that it contains sulphides that segregated from undepleted magma at high R-factors. The upper part of the Unit has  $[Cu/Pd]_n$  greater than unity, indicating that the parent magma may have undergone a previous sulphide segregation event during which the PGE were depleted. The GN Unit has the highest  $[Cu/Pd]_n$  ratios (Fig. 5.6.). This indicates that it crystallized from PGE-depleted magma. Note that the top-chill has similar patterns as the cumulates. The UGAB has low PGE contents,  $[Cu/Pd]_n$  slightly below unity (Fig. 5.6.). This indicates that the rocks have little sulphide and crystallized from a parent magma that was relatively undepleted or moderately depleted in PGE.

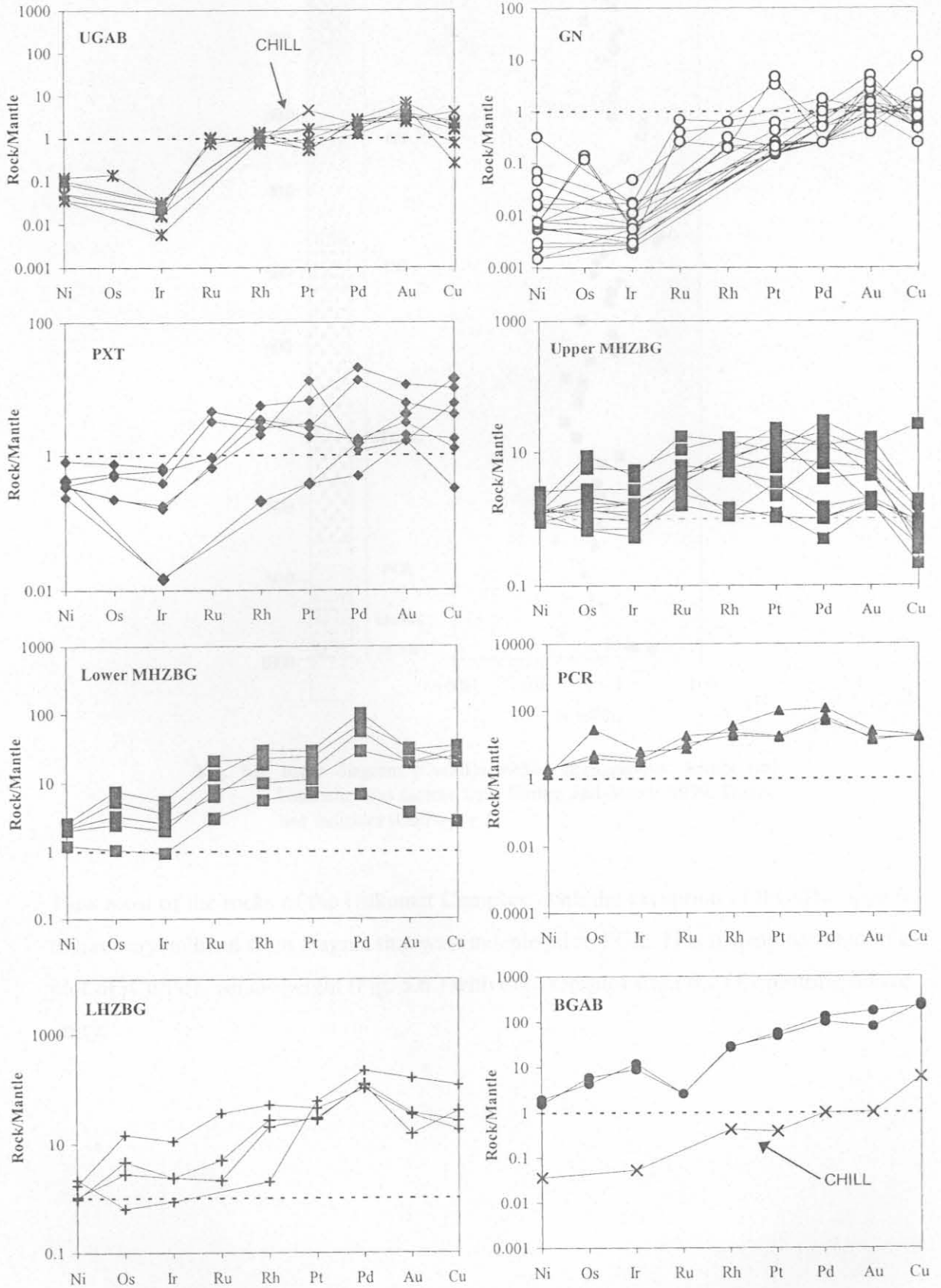


Fig. 5.5. PGE variation through the Complex. Normalization factors from Barnes and Maier (1999).

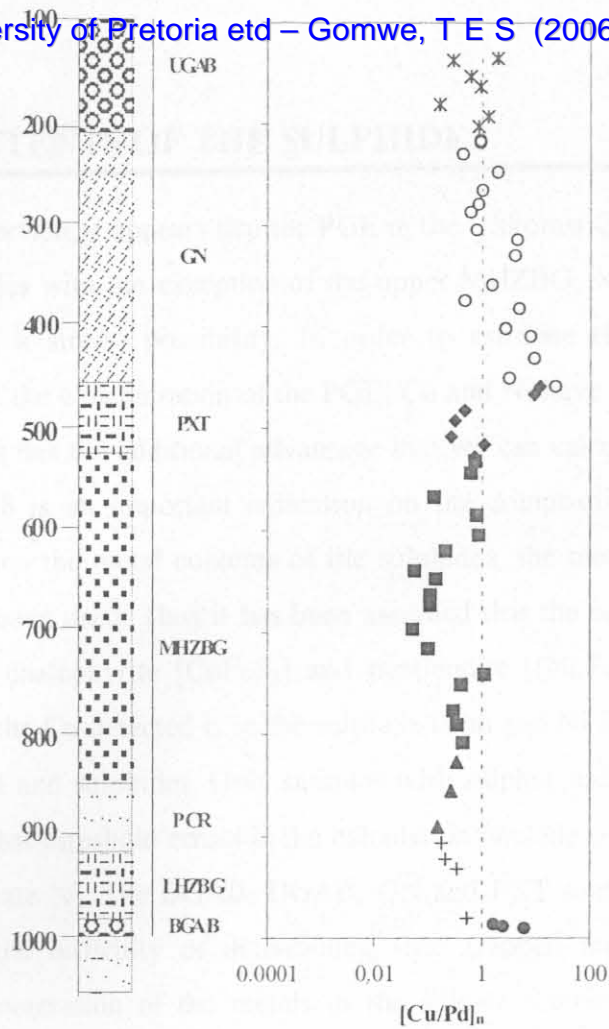


Fig. 5.6. Ratio diagram  $[Cu/Pd]_n$  versus stratigraphic height (m) Normalization factors from Barnes and Maier, 1999. Dotted line indicates  $[Cu/Pd]_n = 1$ .

Thus most of the rocks of the Uitkomst Complex, with the exception of the GN, appear to have crystallized from magma that was undepleted in PGE. This is demonstrated in a plot of  $[Cu/Pd]_n$  versus height (Fig. 5.6.) with only samples from the GN plotting above unity.



## 6. METAL CONTENTS OF THE SULPHIDES

---

From the previous section, it appears that the PGE in the Uitkomst Complex are largely governed by sulphides with the exception of the upper MHZBG, where PGM, mss or chromite control is a strong possibility. In order to estimate the R-factor during sulphide segregation the concentration of the PGE, Cu and Ni have been normalised to 100% sulphide. This has the additional advantage that we can calculate Cu/Ni ratio of the sulphides, which is an important indication on the composition of the parental magma. In calculating the metal contents of the sulphides, the method of Barnes and Francis (1995) has been used. Thus it has been assumed that the sulphides are mainly pyrrhotite  $[\text{Fe}_{1-x}\text{S}]$ , chalcopyrite  $[\text{CuFeS}_2]$  and pentlandite  $[(\text{Ni,Fe})_8\text{S}_9]$ . It is further assumed that all of the Cu detected is in the sulphide form and Ni is hosted by olivine, trapped silicate melt and sulphides. Only samples with sulphur values above 0.1 were selected, as below that threshold errors in the calculation become significant due to the contribution of silicate Ni. The BGAB, UGAB, GN and PXT samples have not been calculated due to the difficulty of determining their trapped melt component. In calculating the concentration of the metals in the silicate fraction of the remaining samples, Bushveld B1 magma has been assumed as parental magma to the Uitkomst Complex.

All Fe in the rocks was initially reported as  $\text{Fe}_2\text{O}_3$ . This is recalculated to allow for Fe in sulphides ( $\text{Fe}_s$ ):

$$\text{Fe}_s = 1.527 \times \text{S} - 0.6592 \times (\text{Cu} - \text{Cu}_{\text{sil}}) - 0.5285 \times (\text{Ni} - \text{Ni}_{\text{sil}}) \quad (1)$$

Cu contents of the silicates are largely represented by trapped melt. B1 magma has about 60 ppm Cu, and the proportion of trapped melt has been estimated as  $(\text{Zr}_{(\text{wr})} / \text{Zr}_{(\text{B1})}) \times 100$ . Nickel contents of the Uitkomst silicates are largely governed by trapped melt and by olivines. Olivine compositions have been determined by C. Li and are given in Appendix IV. The recalculation factor for 100% sulphide (F) is:

$$F = 100 / \{ \text{Fe}_s + \text{S} + (\text{Ni} - \text{Ni}_{\text{sil}}) + (\text{Cu} - \text{Cu}_{\text{sil}}) \} \quad (2)$$

The sulphide normalized metal contents are listed in Appendix IV. All chalcophile elements are then multiplied by the factor (F), less the silicate component as in equations 3, 4 and 5.

$$Ni_{sul} = \{Ni_{anal} - Ni_{sil}\} \times F \quad (3)$$

$$Cu_{sul} = \{Cu_{anal} - Cu_{sil}\} \times F \quad (4)$$

$$PGE_{sul} = \{PGE_{anal} - PGE_{sil}\} \times F \quad (5)$$

Based on the normalized metal data we can estimate the R-factors that applied during sulphide segregation based on the following equation (Maier *et al.*, 1998).

$$C_c = \frac{C_o \times D \times (R+1)}{(R+D)} \quad (6)$$

Which can be rearranged to:

$$R = \frac{C_o D - C_c D}{C_c - C_o D} \quad (7)$$

$C_o$  and  $C_c$  are the concentration of the metal in the initial silicate melt and the sulphide melts, respectively. For the sulphide-rich BGAB, LHZBG and PCR R-factors of between 600 and 1 000 can be calculated. Sulphide-normalised Cu/Ni ratios are plotted in Figure 6.1. For most samples, Cu/Ni varies between about 0.2 and 3, broadly in agreement with crystallization from Bushveld B1 magma (Table 3).

There are two peaks in the Cu/Ni ratio, just below 700 m and at about 580 m, coinciding with two sulphide poor samples of the MHZBG and suggesting that the high values are due to uncertainty in the estimation of silicate Ni.

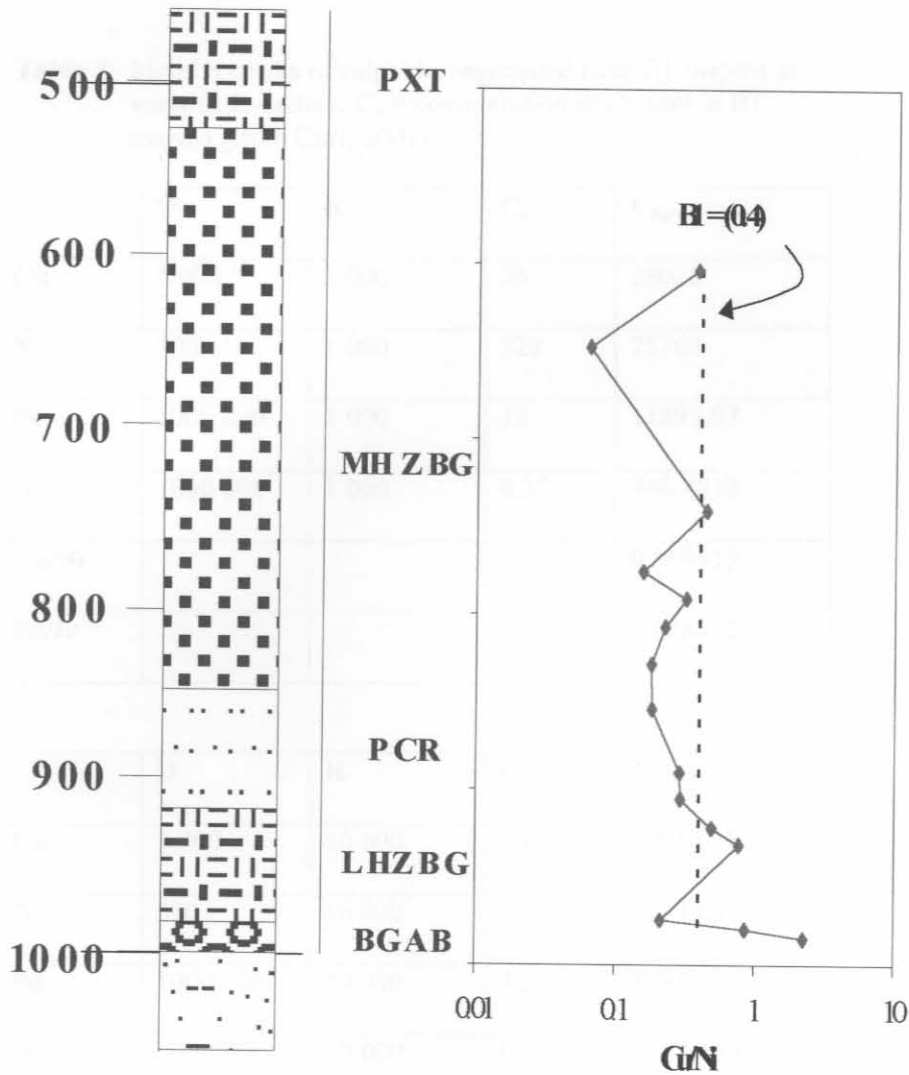


Fig. 6.1 Ratio of Sulphide normalized Cu/Ni versus stratigraphic height (m)

Based on the available data it appears that the PGE in the BGAB, PCR, LHZBG and lower MHZBG appear to be largely controlled by sulphides that segregated at R-factors of around 1000 from undepleted magmas.

The PGE in the upper MHZBG appear to be additionally controlled by PGM possibly associated with disseminated chromite. The PGE in the PXT and GN Units are largely

controlled by metal-poor sulphides that segregated from PGE depleted magma, or by trapped silicate melt undepleted in noble metals in the case of the GN Unit.

**Table 3.** Metal contents of sulphides segregated from B1 magma at variable R-factors.  $C_o$  = concentration of element in B1 magma (from Curl, 2001)

	<b>D</b>	<b>R</b>	<b>C<sub>o</sub></b>	<b>C<sub>Sulf</sub></b>
<b>Cu</b>	1 000	1 000	56	28028
<b>Ni</b>	300	1 000	328	75768
<b>Pd</b>	1000 000	1 000	12	11893.07
<b>Ir</b>	1000 000	1 000	0.35	346.8812
<b>Cu/Ni</b>				0.369919
<b>Pd/Ir</b>				34.28572

	<b>D</b>	<b>R</b>	<b>C<sub>o</sub></b>	<b>C<sub>Sulf</sub></b>
<b>Cu</b>	1 000	10 000	56	50914.18
<b>Ni</b>	300	10 000	328	95543.53
<b>Pd</b>	1000 000	10 000	12	109101.8
<b>Ir</b>	1000 000	10 000	0.35	3182.136
<b>Cu/Ni</b>				0.532890
<b>Pd/Ir</b>				34.28571

## 7. Sm-Nd ISOTOPIC GEOCHEMISTRY

### 7.1. Introduction

Neodymium occurs as several stable isotopes in nature, i.e.  $^{142}\text{Nd}$  to  $^{148}\text{Nd}$  and  $^{150}\text{Nd}$ .  $^{143}\text{Nd}$  is the decay product of  $^{143}\text{Sm}$  ( $\lambda = 6.54 \times 10^{-11}\text{a}^{-1}$ ) (DePaolo, 1988). As a result, the amount of  $^{143}\text{Nd}$ , and the proportion of  $^{143}\text{Nd}$  relative to other isotopes of Nd increases with time, within any rock or mineral that contains the mother element, Sm. For bulk earth these relationships can be illustrated by means of a schematic isotope growth curve (Fig. 7.1.). Clearly, primary partial melts of the upper mantle will have progressively increasing initial  $^{143}\text{Nd}/^{144}\text{Nd}$  ratios with decreasing age.

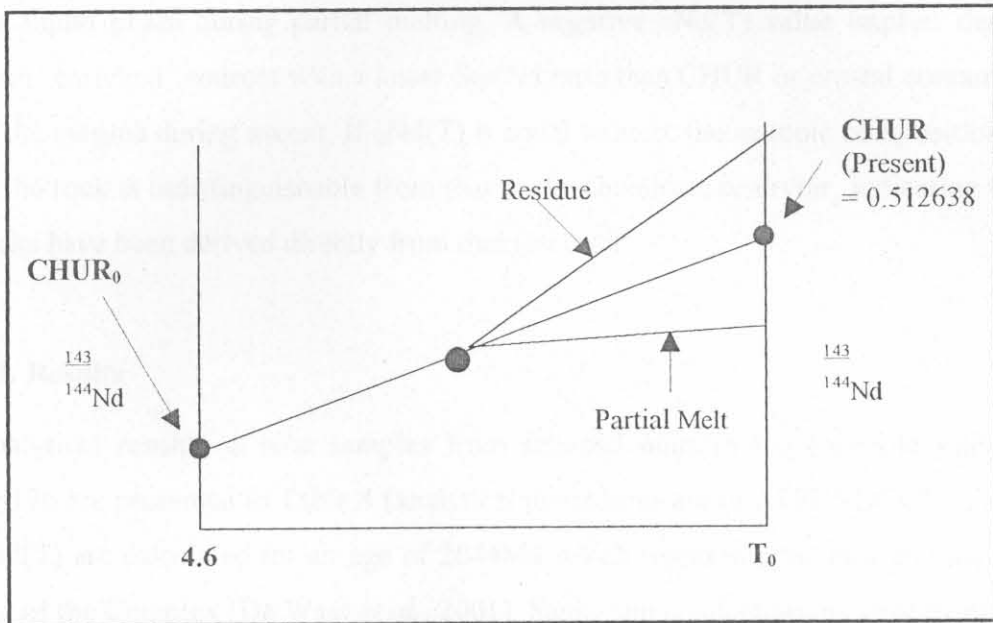


Fig.7.1. The change of  $^{143}\text{Nd}/^{144}\text{Nd}$  ratio with time from 4.6 Ga to the present ( $T_0$ ) in a chondritic uniform reservoir (CHUR) that undergoes partial melting.

During partial melting of the mantle LREE behave more incompatibly than HREE. As a result, the mother isotope  $^{147}\text{Sm}$  tends to be concentrated relative to  $^{143}\text{Nd}$  in the residue, whereas  $^{143}\text{Nd}$  is relatively concentrated in the partial melts (Fig. 7.1.). Partial melts of previously depleted mantle will have high initial  $^{143}\text{Nd}/^{144}\text{Nd}$  ratios relative to  $\text{CHUR}_T$ , while mantle melts that interact with older crust, or partial melts from enriched lithospheric mantle sources, will have low  $^{143}\text{Nd}/^{144}\text{Nd}$  ratios relative to

CHUR<sub>T</sub>. The parameter that defines the comparison between the sample and the chondritic mantle is referred to as εNd(T):

$$\epsilon\text{Nd}(T) = \left[ \frac{(^{143}\text{Nd}/^{144}\text{Nd})}{(^{143}\text{Nd}/^{144}\text{Nd})_{\text{CHUR}}} - 1 \right] \times 10^4 \quad (8)$$

Thus, εNd(T) values may provide information about the magma source. Positive εNd(T) values imply that the magma came from “depleted” sources having higher Sm/Nd ratios than CHUR, that is, the rocks were derived from residual solids in the reservoir after magma had been extracted at an earlier time. These reservoirs are depleted in large ion lithophile (LIL) elements that are preferentially partitioned into the liquid phase during partial melting. A negative εNd(T) value implies derivation from “enriched” sources with a lower Sm/Nd ratio than CHUR or crustal contamination of the magma during ascent. If εNd(T) is equal to zero, the isotopic composition of Nd in the rock is indistinguishable from that in the chondritic reservoir, indicating that the rocks have been derived directly from that reservoir.

### 7.1. Results

Analytical results on nine samples from selected units in the borehole intersection SH176 are presented in Table 4 (analytical procedures are in APPENDIX I). Values of εNd(T) are calculated for an age of 2044Ma which represents the best estimate of the age of the Complex (De Waal *et al.*, 2001). Samarium concentrations vary from 0.66 to about 7ppm and Nd concentrations between 4.4 and 39.7ppm. There is a positive correlation between Sm and Nd (Fig. 7.2.(a)) with sample SH176 UP8 of the GN having the highest Sm and Nd values and SH176 UP32 of the PXT having the lowest values (Table 4).

Figure 7.2.(b) shows <sup>143</sup>Nd/<sup>144</sup>Nd plotted versus <sup>147</sup>Sm/<sup>144</sup>Nd. It is evident that the data do not define an isochron, which is best explained by selective crustal contamination of some or all of the Uitkomst rocks. Thus, age estimates by this method would have no geological significance. This model is supported by the εNd(T) values of the samples which range between -3.4 and -7.6 indicative of a significant crustal component.

**Table 4.** Neodymium and strontium isotope data. Epsilon Nd values calculated for an age of 2044Ma

Sample No	Unit	Depth (m)	Nd (ppm)	Sm (ppm)	$^{147}\text{Sm}/^{144}\text{Nd}$	$^{143}\text{Nd}/^{144}\text{Nd}$ (measured)	Error	Nd (T=2044Ma)
SH176UP1	UGAB	135.41	19.1	3.75	0.12449	0.511401	80	-5.4
SH176UP5	UGAB	181.09	12.6	2.48	0.12548	0.511301	9	-7.6
SH176UP8	GN	216.22	39.7	6.99	0.11302	0.511213	13	-5.9
SH176UP19	GN	375.42	12.1	2.26	0.12230	0.511356	8	-5.8
SH176UP23	GN	432.11	8.92	1.89	0.13349	0.511472	11	-6.6
SH176UP26	PXT	459.75	6.88	1.3	0.12873	0.511416	8	-6.7
SH176UP32	PXT	527.04	2.443	0.531	0.13139	0.511336	8	-8.3
SH176UP40	MHZBG	647.6	3.38	0.66	0.14118	0.511648	7	-6.03
SH176UP49	MHZBG	807.04	5.3	1.12	0.12714	0.511486	14	-4.68
SH176UP51	PCR	854.06	4.43	0.88	0.12126	0.511493	37	-3.38
SH176UP60	BGAB	990.29	23.179	5.524	0.14405	0.511438	58	-8.8

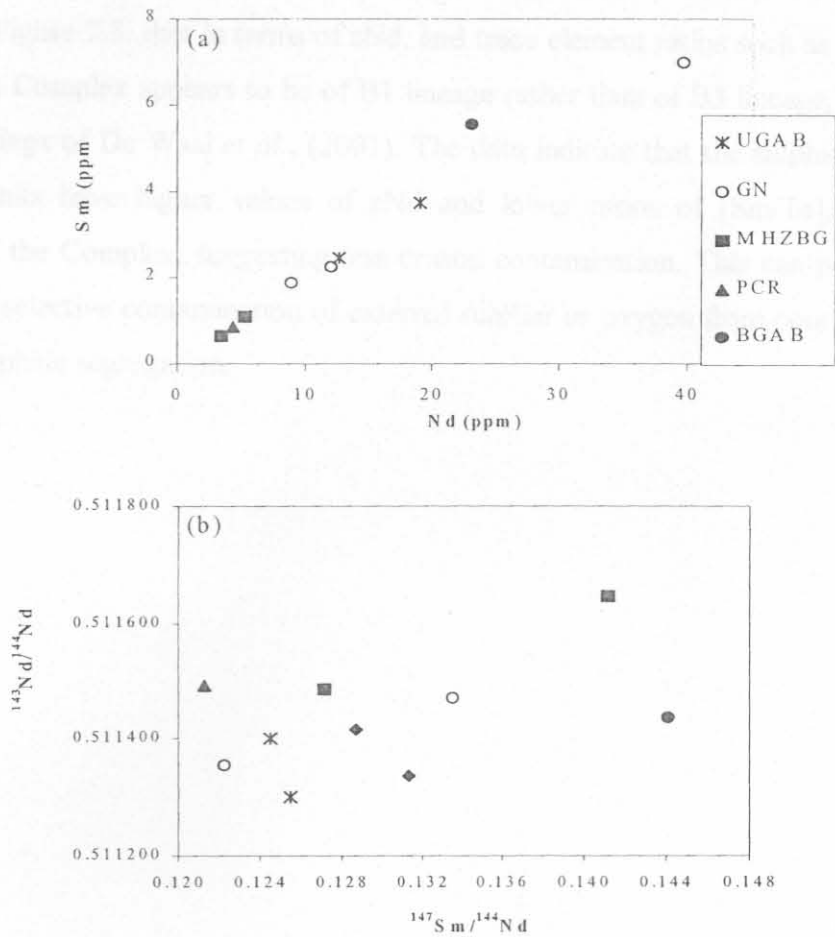


Fig. 7.2. Sm-Nd variation diagrams (a) Sm vs. Nd. (b)  $^{143}\text{Nd}/^{144}\text{Nd}$  versus  $^{147}\text{Sm}/^{144}\text{Nd}$  isochron diagram.

### 7.3. Stratigraphic variation in $\epsilon\text{Nd}$

The  $\epsilon\text{Nd}(T)$  as well as the  $[\text{Sm}/\text{Ta}]_n$  ratios are plotted against stratigraphic height (Fig. 7.3.) to enable comparison with data obtained by Maier *et al.*, (2000) on Bushveld cumulates and parental magmas. These authors showed that the Bushveld Complex was contaminated with progressively more depleted crust. The parental magmas to the Lower Zone (LZ) and Lower Critical Zone (LCZ), i.e. B1 magma, assimilated relatively small amounts of partial melts of undepleted crust that were highly enriched in incompatible trace elements. The Main Zone (MZ) magmas (B3 magma) assimilated larger amounts of residual crust that was less enriched in incompatible trace elements. As a result, B1 magmas and associated cumulates show a higher  $\epsilon\text{Nd}$  (-5 to -6), but are enriched in highly incompatible trace elements relative to B3 magmas and cumulates ( $\epsilon\text{Nd}$  -6.5 to -7.5).



It is seen in Figure 7.3. that in terms of  $\epsilon\text{Nd}$ , and trace element ratios such as  $[\text{Sm}/\text{Ta}]_n$ , the Uitkomst Complex appears to be of B1 lineage rather than of B3 lineage, in accord with the findings of De Waal *et al.*, (2001). The data indicate that the sulphide-bearing rocks and units have higher values of  $\epsilon\text{Nd}$  and lower ratios of  $[\text{Sm}/\text{Ta}]_n$  than the remainder of the Complex, suggesting less crustal contamination. This can possibly be explained by selective contamination of external sulphur or oxygen from country rocks, triggering sulphide segregation.

8. DISCUSSION AND CONCLUSIONS

The objectives of this project were cross-cutting. Firstly I tried to establish whether the Uthmaniyah Complex crystallized as a static system or as a dynamic system in a tectonic setting. Secondly, I placed an emphasis on understanding the tectonic evolution of the crystallized Sm/Sm ratios of the Uthmaniyah Complex and to what extent the patterns of the Uthmaniyah Complex can be compared with the patterns of the Uthmaniyah Complex in the Uthmaniyah Complex of the Uthmaniyah Complex.

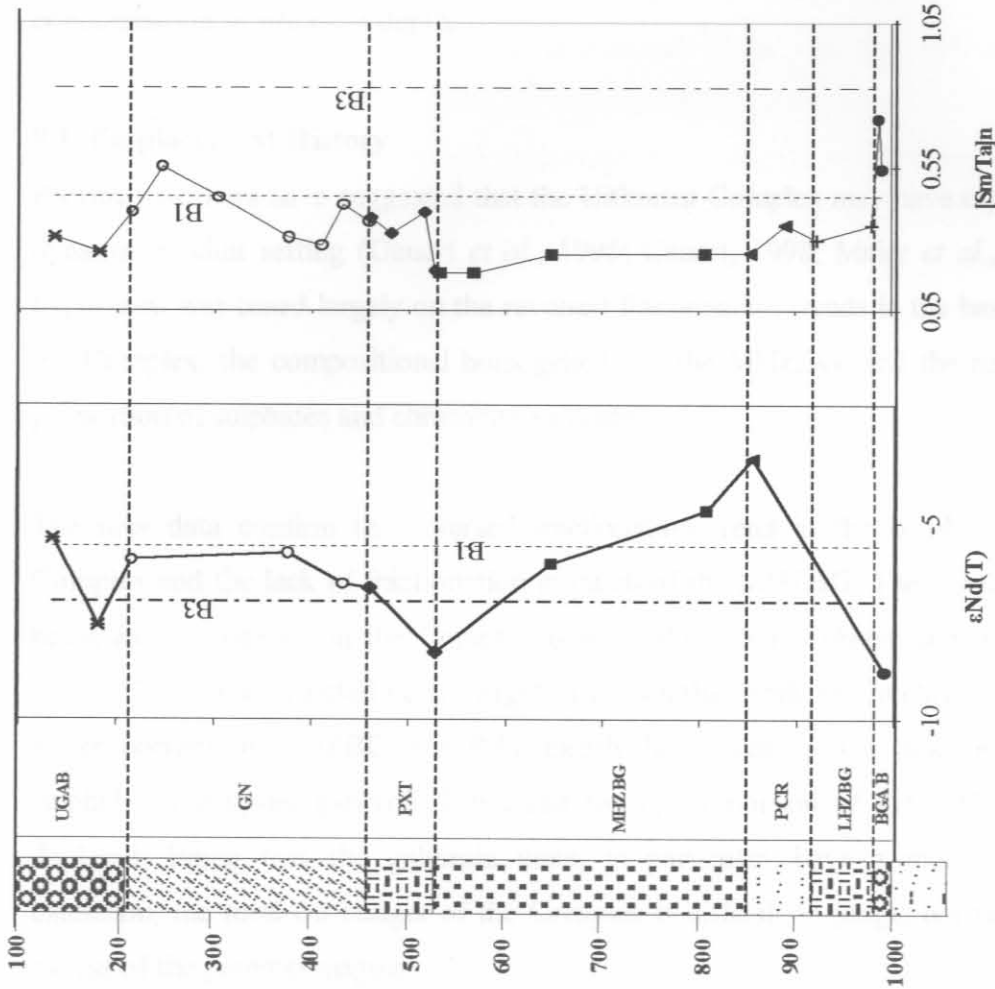


Fig. 7.3. Stratigraphic variation of [Sm/Ta]<sub>n</sub>. Depth is in meters. Average B1 and B3 values are from Curl (2001).

... in an opposite way to what would be expected in a closed system (Fig. 7.2). They decrease with height up to the top of the Uthmaniyah Complex in the Uthmaniyah Complex. P/Ti increases with height indicating that it is more compatible than Ti during crystallization of igneous rocks. This suggests that in the Uthmaniyah Complex, the upper portions of the MEZBG are not related to the underlying Uthmaniyah Complex by means of a